PHYSICAL REVIEW B **96**, 020413(R) (2017)

Long-period helical structures and twist-grain boundary phases induced by chemical substitution in the $Mn_{1-x}(Co,Rh)_xGe$ chiral magnet

N. Martin,[1,*] M. Deutsch,[2] G. Chaboussant,[1] F. Damay,[1] P. Bonville,[3] L. N. Fomicheva,[4] A. V. Tsvyashchenko,[4,5] U. K. Rössler,[6] and I. Mirebeau[1]

[1]*Laboratoire Léon Brillouin, CEA, CNRS, Université Paris-Saclay, CEA Saclay 91191 Gif-sur-Yvette, France*

[2]*Université de Lorraine, Laboratoire CRM2,UMR UL-CNRS 7036, 54506 Vandoeuvre-les-Nancy, France*

[3]*SPEC, CEA, CNRS, Université Paris-Saclay, CEA-Saclay, 91191 Gif-sur-Yvette, France*

[4]*Vereshchagin Institute for High Pressure Physics, Russian Academy of Sciences, 142190 Troitsk, Moscow, Russia*

[5]*Skobeltsyn Institute of Nuclear Physics, MSU, Vorob'evy Gory 1/2, 119991 Moscow, Russia*

[6]*IFW Dresden, PO Box 270116, 01171 Dresden, Germany*

(Received 21 February 2017; revised manuscript received 1 June 2017; published 21 July 2017)

We study the evolution of helical magnetism in MnGe chiral magnet upon partial substitution of Mn for 3*d*-Co and 4*d*-Rh ions. At high doping levels, we observe spin helices with very long periods—more than ten times larger than in the pure compound—and sizable ordered moments. This behavior calls for a change in the energy balance of interactions leading to the stabilization of the observed magnetic structures. Strikingly, neutron scattering unambiguously shows a double periodicity in the observed spectra at $x = 0.5$ and >0.2 for Co- and Rh-doping, respectively. In analogy with observations made in smectic liquid crystals, we suggest that it may reveal the presence of magnetic "twist grain boundary" phases, involving a dense short-range correlated network of magnetic screw dislocations. The dislocation cores are here tentatively described as smooth textures, made of nonradial double-core skyrmions.

DOI: 10.1103/PhysRevB.96.020413

In condensed matter, effects of quenched disorder [1] on an ordered phase can be strikingly different, varying between marginal modifications of phase transitions to the destruction of homogeneous order and the occurrence of disordered, amorphous, or glassy states [2]. Particularly interesting are systems where disorder only partly destroys the ordered state and prompts the appearance of localized defects. Liquid crystals and helium quantum liquids confined in random environments are well studied examples of such systems [3,4].

In chiral helimagnets, helimagnetic structures can arise from the competition of near neighbor interactions between localized spins, leading to a short helical period λ_H comparable to the lattice constant a [5]. For long helical periods ($\lambda_H \gg a$) the free energy is usually described in a continuum model by a functional involving an effective exchange constant $\mathcal{A}$ and two anisotropic terms, i.e., the Dzyaloshinskii-Moriya (DM) interaction $\mathcal{D}$ and the exchange anisotropy $\mathcal{B}$. A hierarchical model [6] leads to a helical magnetic ground state with period $\lambda_H \simeq \mathcal{A}/\mathcal{D}$. In a random system, $\mathcal{A}$, $\mathcal{D}$, and $\mathcal{B}$ are spatially varying but with fixed distributions. Thanks to proper metric rescaling of space, quenched disorder can formally be canceled, as long as it does not lead to an inversion of the locally favored twisting. Its leading effect comes from random anisotropy, so that a ground state helical structure should basically be preserved, while randomness would only modify the local wavelength, the rotation axis and, in some cases, the propagation direction of spin spirals.

Long period helimagnetic states are closely related to one-dimensional smectic liquid crystals [7]. In pure form, they can form double twisted solitonic structures—now known as *skyrmions*—on length scales much larger than lattice spacings and akin to cholesteric liquid crystals. The equivalence of the long distance behavior of the helimagnetic ground state with smectic liquid crystals allows us to use basic theories about smectics in random anisotropic media [3,8], which state that any anisotropic disorder destroys homogeneous long range order. It suggests that, as in smectic crystals, spin helices in chiral systems could be modified by the penetration of dislocations [8], the density of which increasing with the amount of disorder, yielding twist grain boundary (TGB) phases [9].

Here, we use alloys of the cubic magnet MnGe to investigate the influence of quenched disorder on the chiral helimagnetic ground state. We have substituted Mn for 3*d*-Co or 4*d*-Rh ions and focused on compositions belonging to the Mn rich side ($x \leqslant 0.5$) of the $Mn_{1-x}(Co,Rh)_xGe$ series. In both cases, we observe that doping induces helical structures with very long periods (up to $\simeq$550 Å, as compared to $\simeq$30 Å for pure MnGe [10]) and sizable ordered moments. Moreover, we show that they differ from harmonic helices by the presence of *two* magnetic diffraction peaks, calling for an additional periodicity. We propose that it may reveal the presence of magnetic TGB phases, as discussed in the last part of this paper.

In order to follow the evolution of the magnetic structure in $Mn_{1-x}(Co,Rh)_xGe$, neutron powder diffraction measurements were performed on the G4.1 instrument at the Laboratoire Léon Brillouin (LLB) using an incident wavelength $\lambda = 2.428$ Å. The obtained powder patterns show satellites of the nuclear Bragg reflections, a hallmark of helimagnetic long-range ordering. In pure MnGe, the intense satellite of the $Q = 0$ Bragg peak, clearly visible at low angles, coexists with much weaker satellites at larger angles [10]. Its evolution with increasing Co content is shown in Fig. 1(a) at base temperature. With increasing x, the helimagnetic satellite broadens, its intensity strongly decreases, and its position moves towards lower Q values. For $x = 0.5$, the peak has evaded from the diffraction window. In $Mn_{1-x}Rh_xGe$, the intensity of the

*nicolas.martin@cea.fr

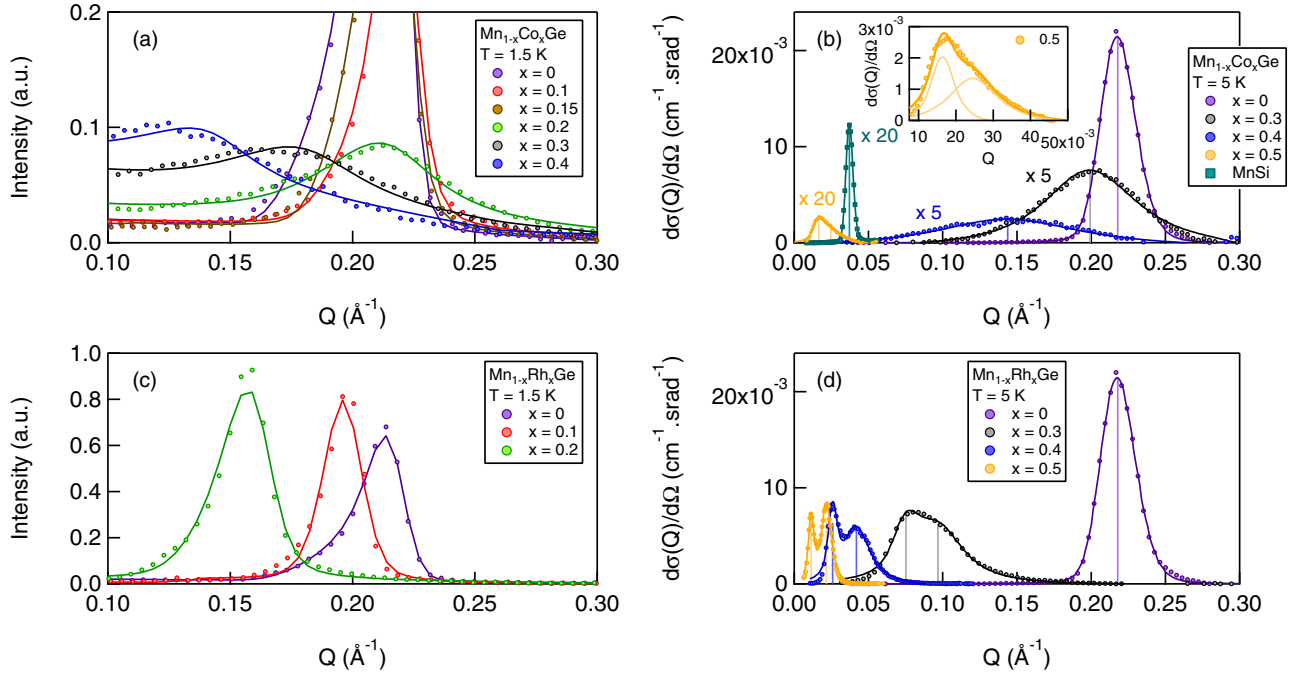

FIG. 1. Evolution of the helimagnetic peak in $Mn_{1-x}Co_xGe$ (a) and $Mn_{1-x}Rh_xGe$ (c) upon doping at $T = 1.5$ K, as measured by neutron powder diffraction. For each concentration a pattern measured at 300 K was subtracted to eliminate background. For display purposes, patterns were calibrated to the intensity of the (110) nuclear reflection. Small-angle neutron scattering patterns of $Mn_{1-x}Co_xGe$ (b) and $Mn_{1-x}Rh_xGe$ (d) taken at $T = 5$ K. One can note (i) the large increase of the helical wavelength as a function of x and (ii) the emergence of a second peak for $x = 0.5$ (Co) [see also inset of (b)] and $x > 0.2$ (Rh). In all panels, solid lines are fit curves as described in the text.

satellite is not decreasing, but its position shifts very quickly with increasing x and it disappears from the diffraction window for $x > 0.2$ [Fig. 1(c)].

In both cases, measurements covering a lower Q range are thus needed to follow the evolution of the magnetic structure. In that respect, small-angle neutron scattering (SANS) is an ideal method since it can access momentum transfers as small as a few 10^{-4} Å^{-1}. Experiments were performed on the spectrometers PA20 and PAXY [11,12] of the LLB, using incident wavelengths 4.46 and 6 Å, and sample-to-detector distances ranging between 2 and 10 m. Spectra were corrected for detector efficiency and calibrated cross sections were obtained by taking sample thickness, transmission, and incident neutron flux into account [13]. In $Mn_{1-x}Co_xGe$, the helimagnetic peak is now clearly evidenced for $x = 0.5$ [Fig. 1(b)]. Its asymmetric lineshape is best accounted for by a sum of two peaks (inset of Fig. 1 b). In $Mn_{1-x}Rh_xGe$, we observe a magnetic signal for $x > 0.2$ [Fig. 1(d)]. Moreover, thanks to the symmetric and narrow line shape of the resolution function, we observe a resolved two peak structure. The appearance of a second peak calls for a new periodicity in the system occurring at high doping, namely at $x = 0.5$ and $x > 0.2$ for Co and Rh substitutions, respectively.

In the data treatment, we assumed helical order with magnetic moments on the Mn sites only, propagating along (001) axes, as for pure MnGe. Diffraction patterns were described in the cubic space group $P2_13$, with a helical wave vector $\mathbf{Q}_H = (0,0,Q_H)$. Combined nuclear and magnetic refinements provide the helical wave number Q_H, the inverse correlation length κ_H and the ordered moment m. In the SANS case, parameters describing magnetic order are obtained by assuming an Ornstein-Zernike form for the scattering function $\mathcal{S}(Q)$ (with peak position Q_H and half-width at half-maximum κ_H), convolved with the calculated resolution function $\mathcal{R}(Q)$ [13]. We have calibrated m on an absolute scale by measuring the integrated intensity of the helical peak in MnGe ($m = 1.85\ \mu_B$/Mn) and MnSi ($m = 0.4\ \mu_B$/Mn) powder samples [13]. This analysis strategy is fully general and is found to reproduce very well magnetic SANS patterns for all studied compositions. The helix pitch $\lambda_H = 2\pi/Q_H$, coherence length $\xi_H = 1/\kappa_H$ and Mn ordered moment m determined at base temperature are reported in Fig. 2.

The first striking feature is the huge increase of the helix pitch for large x, reaching 380 and 550 Å at $x = 0.5$ for Co- and Rh-doping respectively. Such behavior calls for of a deep change in the energy balance of magnetic interactions upon substitution. It suggests that undoped MnGe actually realizes a frustration driven helix [5], where the short helical period stems from the competition of near neighbor ferro- (FM) and antiferromagnetic (AFM) interactions [14] (or equivalently from RKKY interaction oscillating in sign). Conversely, the long-period helices observed at high Co/Rh doping must be governed by a smaller ratio of AFM-to-FM exchange, together with a fine tuning of the average FM exchange by a small DM anisotropy [6]. We note that the DM interaction may change in magnitude with doping as shown in $Mn_{1-x}Fe_xGe$, both experimentally [15,16] and theoretically [17–19]. More elaborate calculations including all interactions are necessary to check the above scenario for $Mn_{1-x}(Co,Rh)_xGe$.

We now focus on the x dependence of the ordered moment. This is an absolute derivation of this quantity from SANS data in B20 materials. The long range ordered moment is

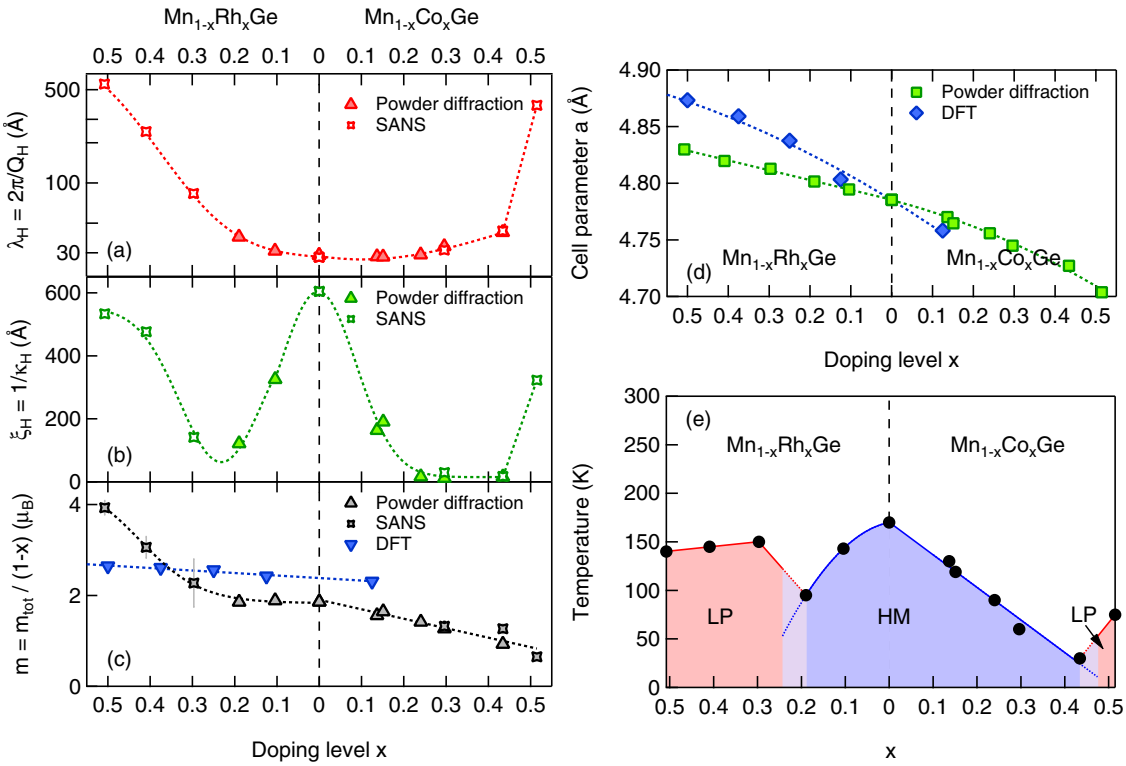

FIG. 2. Doping dependence of the helical wavelength λ_H (a), the coherence length ξ_H (b) and the ordered magnetic moment m (c) in $Mn_{1-x}(Co,Rh)_xGe$ as determined by powder neutron diffraction and small-angle scattering. In panel (c), results of *ab initio* calculations of the local Mn moment are shown for comparison. (d) Cubic lattice constant of $Mn_{1-x}(Co,Rh)_xGe$ versus doping x determined by neutron powder diffraction at $T = 1.5$ K. (e) Magnetic phase diagram of $Mn_{1-x}(Co,Rh)_xGe$ inferred from neutron scattering (Néel temperature, T_N). At low temperature, below $x \simeq 0.45$ for Co doping and $x \simeq 0.25$ for Rh doping, a standard helimagnetic (HM) state is stabilized. At higher values of x, more complex long-period magnetic structures are observed (LP).

determined *per crystallographic site*, namely one cannot have access to the moment on Mn and Co/Rh atoms separately since they share the same Wyckoff site. The quantity $m = m_{tot}/(1-x)$ (where m_{tot} is the ordered moment per formula unit) is equal to the ordered Mn moment if Co/Rh and Ge atoms bear no moment. As seen in Fig. 2(c), m decreases with increasing Co content but strongly increases in $Mn_{1-x}Rh_xGe$ for $x > 0.2$. In order to acquire a better understanding of this phenomenon, *ab initio* calculations have been performed in $Mn_{1-x}(Co,Rh)_xGe$ systems, using a $2 \times 1 \times 1$ supercell containing eight formula units [13]. Small magnetic moments of less than $\simeq 0.5\ \mu_B$ are found on Co, Rh, and Ge sites. The calculated Mn moment shows a moderate correlation with the lattice parameter, but the anomalous increase observed in $Mn_{1-x}Rh_xGe$ for $x > 0.2$ is not predicted by theory. We attribute this either to a Mn spin transition favored by lattice expansion [20,21] or to large induced moments on the Rh sites.

The magnetic phase diagram of $Mn_{1-x}(Co,Rh)_xGe$ ($x \leqslant 0.5$) is shown in Fig. 2(e). Co-doping is more prone to destabilizing long-range order than Rh doping, as seen by the x dependence of the ordering temperature T_N. Susceptibility data reflect the same behavior [13]. Strikingly, in both systems, a doping-induced transition is observed from a helimagnetic state towards a new type of magnetic structure, corresponding to an additional peak in the SANS patterns.

We now focus on the double periodicity shown by the LP structures at high doping. Its observation in the two systems suggests its intrinsic character. The second peak is neither a higher order harmonics of the helical order, excluding a description by anisotropy induced square modulations of the local magnetization [22], nor due to multiple Bragg scattering. Our refinements of the crystal structure also exclude a macroscopic phase separation, since all samples remain in a single cubic phase without noticeable broadening of the measured nuclear peaks. Moreover the two peaks vary with T and x in correlated ways [13], which would not occur for a macroscopic phase separation. Having eliminated all trivial explanations for this complex texture, we propose that above some critical concentration, quenched disorder and Co/Rh substitution induce magnetic regions within which the LP spirals develop and change orientation.

It is well known that spatially modulated phases with very long periods can be stabilized by competing interactions. Numerous examples can be found in nature, such as stripe domain patterns in layered superconductors, ferroelectrics, Langmuir films, ferrofluids, or magnetic garnets. Nonlocal interactions associated with electric polarization, magnetization, or elastic strains can be the source of such competitions, the modulation period λ_{mod} being related to the ratio of the coefficients for the competing energy terms in a Landau formalism [23–25]. Even if a precise mechanism for the formation of a complex LP structure is far beyond our goal, we propose to describe it as due to magnetic TGB phases, predicted [9] and evidenced [26] in smectic liquid crystals.

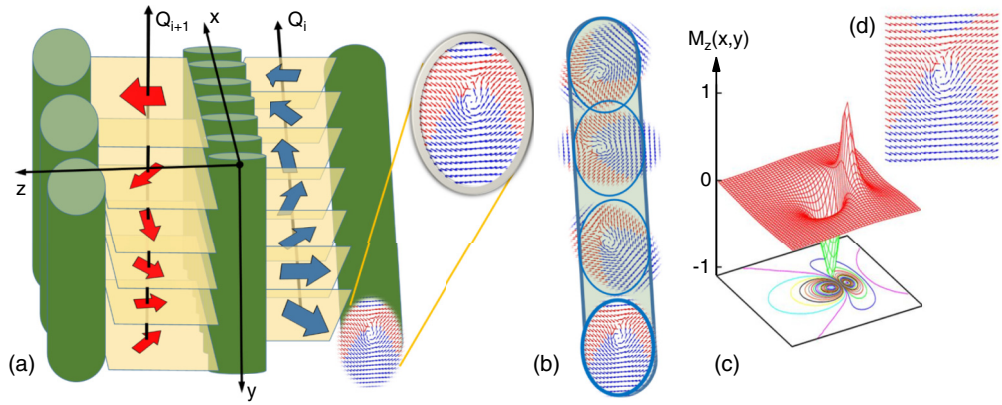

FIG. 3. (a) Schematic view of the proposed twist grain boundary (TGB) structure in a chiral helimagnet. (b) Internal structure of a screw dislocation made of stacked double core skyrmions. (c),(d) Cross section of a double core skyrmion: (c) out of plane magnetization component M_Z and (d) projection of the in-plane component, showing a narrowly coupled vortex-antivortex configuration. The ferromagnetic vector **m** describes a full sweep over the 4π surface of the sphere. The projection of **m** forms a vortex-antivortex pair in the plane of the cross section perpendicularly to the dislocation line. At the locations of the vortex singularities **m** is exactly perpendicular to the plane pointing up and down. Along the dislocation line, the locations of these two extremal values of **m** twist in a corkscrew fashion around each other.

In chiral systems realizing TGB phases, quasicrystalline dislocations can occur in directions perpendicular to the propagation direction of the primary 1D modulations [9]. Here, the balance between exchange and twisting DM term is optimal along the propagation direction of the primary spiral order, but this order is still frustrated and, upon insertion of dislocations, can twist additionally in the perpendicular direction [Fig. 3(a)]. These textures are caused by defect generation through 'penetration of chirality' described by de Gennes in analogy to type II superconductors [27]. A planar arrangement of parallel screw dislocations [in the xy plane, Fig. 3(b)] connects slablike regions of spiral helices with differing propagation directions, and thus, acts as a TGB.

In a first step [13], we speculate that a periodic arrangements of these TGBs could occur, yielding a secondary modulation, in direct analogy with the smectic case [28]. In contrast to smectics, however, the lateral twisting of the DM spirals should take place on the length scale of the twisting period λ_H itself. Therefore, the dislocation cores should occupy a large volumic fraction, as supported by the large intensity of the secondary peak. In a second step, we consider the internal structure of the magnetic TGB, which should be smooth and defect-free in terms of the ferromagnetic order, avoiding the high energy cost of forming singular defects (Bloch points). To comply with this constraint, we describe the dislocation core as a smooth texture of a nonradial double core and singly charged skyrmion [Figs. 3(c) and 3(d)]. Such a structure is topologically nontrivial, although the net topological charge is about zero. As discussed in Ref. [13], it should also yield a secondary modulation, at a position related to the size of the core. This would be the case even if the cores are mutually randomly oriented, so that the twisting in the transverse direction occurs in a disordered fashion. In such a case, the propagation vector of the helix could rotate over a full circle on a length scale comparable to the helix period and not in a discrete way as for smectic TGBs.

Finally we notice that after this paper was submitted, topological domain walls analog to liquid crystals have been observed in FeGe [29]. Analogous dislocation structures were also evidenced in cholesteric liquid crystals [30,31]. Recent simulation studies also report such 3D twistings, corresponding to partial penetration of chirality into the 1D spiral [32,33].

In summary, Co/Rh substitution in MnGe induces magnetic structures with very long periods and magnetic moments strongly dependent on the unit cell volume. While the first feature reveals a change in the energy balance of magnetic interactions, from frustrated near neighbor interactions to the hierarchical Bak-Jensen scheme, the second one suggests deep modifications of the material band structure. The double LP structures observed at high doping suggest that strong quenched disorder partly destroys the spiral ground state and stabilizes defects, tentatively described as a 3D TGB-like phase with a dense network of magnetic screw dislocations. Transitions from simple spin spirals to LP structures occur at $x \simeq 0.45$ for $Mn_{1-x}Co_xGe$ and $x \simeq 0.25$ for $Mn_{1-x}Rh_xGe$. Whether this process takes place through a quantum critical point or in a thermally assisted way remains to be checked experimentally.

We thank E. Altynbaev and S. Grigoriev for very insightful discussions, S. Gautrot and V. Thevenot for technical assistance, and A. Bauer for provision of MnSi powder samples. A.V.T. is grateful for the Russian Science Foundation (Grant No. 17-12-01050).

[1] P. W. Anderson, in *Ill Condensed Matter*, Les Houches Session XXXI (1978), edited by R. Balian, R. Maynard, and G. Toulouse (North Holland, Amsterdam, 1979).

[2] A. P. Young, *Spin Glasses and Random Fields* (World Scientific, Singapore, 1997), Vol. 12.

[3] T. Bellini, L. Radzihovsky, J. Toner, and N. A. Clark, Science **294**, 1074 (2001).

[4] G. Volovik, *The Universe in a Helium Droplet* (Oxford University Press, 2003), Vol. 117.

[5] J.-I. Kishine and A. Ovchinnikov, *Solid State Physics* (Academic Press, 2015), Vol. 66, pp. 1–130.
[6] P. Bak and M. H. Jensen, J. Phys. C: Sol. St. Phys. **13**, L881 (1980).
[7] L. Radzihovsky and T.C. Lubensky, Phys. Rev. E. **83**, 051701 (2011).
[8] L. Radzihovsky and J. Toner, Phys. Rev. B **60**, 206 (1999).
[9] S. R. Renn and T. C. Lubensky, Phys. Rev. A **38**, 2132 (1988).
[10] O. L. Makarova, A. V. Tsvyashchenko, G. Andre, F. Porcher, L. N. Fomicheva, N. Rey, and I. Mirebeau, Phys. Rev. B **85**, 205205 (2012).
[11] G. Chaboussant, S. Désert, P. Lavie, and A. Brûlet, J. Phys.: Conf. Series **340**, 012002 (2012).
[12] G. Chaboussant, S. Désert, and A. Brûlet, Eur. Phys. J.: Spec. Top. **213**, 313 (2012).
[13] See Supplemental Material at http://link.aps.org/supplemental/10.1103/PhysRevB.96.020413 for more details about sample preparation, magnetic measurements, neutron scattering data analysis, *ab initio* calculations, and the proposed model of magnetic 'twist grain boundary' phases, which includes Refs. [34–46].
[14] V. A. Chizhikov and V. E. Dmitrienko, Phys. Rev. B **88**, 214402 (2013).
[15] S. V. Grigoriev, N. M. Potapova, S.-A. Siegfried, V. A. Dyadkin, E. V. Moskvin, V. Dmitriev, D. Menzel, C. D. Dewhurst, D. Chernyshov, R. A. Sadykov *et al.*, Phys. Rev. Lett. **110**, 207201 (2013).
[16] K. Shibata, X. Yu, T. Hara, D. Morikawa, N. Kanazawa, K. Kimoto, S. Ishiwata, Y. Matsui, and Y. Tokura, Nat. Nanotechnol. **8**, 723 (2013).
[17] J. Gayles, F. Freimuth, T. Schena, G. Lani, P. Mavropoulos, R. A. Duine, S. Blügel, J. Sinova, and Y. Mokrousov, Phys. Rev. Lett. **115**, 036602 (2015).
[18] T. Koretsune, N. Nagaosa, and R. Arita, Sci. Rep. **5**, 13302 (2015).
[19] T. Kikuchi, T. Koretsune, R. Arita, and G. Tatara, Phys. Rev. Lett. **116**, 247201 (2016).
[20] M. Deutsch, O. L. Makarova, T. C. Hansen, M. T. Fernandez-Diaz, V. A. Sidorov, A. V. Tsvyashchenko, L. N. Fomicheva, F. Porcher, S. Petit, K. Koepernik *et al.*, Phys. Rev. B **89**, 180407(R) (2014).
[21] N. Martin, M. Deutsch, J.-P. Itié, J.-P. Rueff, U. K. Rössler, K. Koepernik, L. N. Fomicheva, A. V. Tsvyashchenko, and I. Mirebeau, Phys. Rev. B **93**, 214404 (2016).
[22] Y. A. Izyumov, Sov. Phys. Usp. **27**, 845 (1984).
[23] M. Seul and D. Andelman, Science **267**, 476 (1995).
[24] D. I. Khomskii and K. I. Kugel, Europhys. Lett. **55**, 208 (2001).
[25] G. Malescio and G. Pellicane, Nat. Mater. **2**, 97 (2003).
[26] J. W. Goodby, M. A. Waugh, S. M. Stein, E. Chin, R. Pindak, and J. S. Patel, Nature (London) **337**, 449 (1989).
[27] P. De Gennes, Solid State Commu. **10**, 753 (1972).
[28] L. Navailles, R. Pindak, P. Barois, and H. T. Nguyen, Phys. Rev. Lett. **74**, 5224 (1995).
[29] P. Schoenherr, J. Müller, L. Köhler, A. Rosch, N. Kanazawa, Y. Tokura, M. Garst, and D. Meier, arXiv:1704.06288.
[30] Y. Bouligand and M. Kléman, J. Phys. **31**, 1041 (1970).
[31] J. Rault, Philos. Mag. **30**, 621 (1974).
[32] F. N. Rybakov, A. B. Borisov, and A. N. Bogdanov, Phys. Rev. B **87**, 094424 (2013).
[33] A. O. Leonov, T. L. Monchesky, J. C. Loudon, and A. N. Bogdanov, J. Phys.: Condens. Matter **28**, 35LT01 (2016).
[34] M. Deutsch, P. Bonville, A. V. Tsvyashchenko, L. N. Fomicheva, F. Porcher, F. Damay, S. Petit, and I. Mirebeau, Phys. Rev. B **90**, 144401 (2014).
[35] N. Martin, M. Deutsch, F. Bert, D. Andreica, A. Amato, P. Bonfà, R. De Renzi, U. K. Rößler, P. Bonville, L. N. Fomicheva *et al.*, Phys. Rev. B **93**, 174405 (2016).
[36] N. Kanazawa, Y. Onose, T. Arima, D. Okuyama, K. Ohoyama, S. Wakimoto, K. Kakurai, S. Ishiwata, and Y. Tokura, Phys. Rev. Lett. **106**, 156603 (2011).
[37] E. Altynbaev, S.-A. Siegfried, V. Dyadkin, E. Moskvin, D. Menzel, A. Heinemann, C. Dewhurst, L. Fomicheva, A. Tsvyashchenko, and S. Grigoriev, Phys. Rev. B **90**, 174420 (2014).
[38] R. Viennois, C. Reibel, D. Ravot, R. Debord, and S. Pailhès, Europhys. Lett. **111**, 17008 (2015).
[39] J. Rodrìguez-Carvajal, Physica B **192**, 55 (1993).
[40] G. Caglioti, A. Paoletti, and F. Ricci, Nucl. Instrum. **3**, 223 (1958).
[41] A. Brûlet, D. Lairez, A. Lapp, and J.-P. Cotton, J. Appl. Crystallogr. **40**, 165 (2007).
[42] J. G. Barker and D. F. R. Mildner, J. Appl. Crystallogr. **48**, 1055 (2015).
[43] F. Cser, J. Appl. Polym. Sci. **80**, 358 (2001).
[44] U. K. Rössler, J. Phys.: Conf. Ser. **391**, 012104 (2012).
[45] M. Hennion, I. Mirebeau, F. Hippert, B. Hennion, and J. Bigot, J. Magn. Magn. Mater. **54**, 121 (1986).
[46] H. Kawamura and M. Tanemura, J. Phys. Soc. Jpn. **60**, 1092 (1991).